Talanta 85 (2011) 1760–1765

Contents lists available at ScienceDirect

Talanta

journal homepage: www.elsevier.com/locate/talanta

Nanoliter droplet array for microRNA detection based on enzymatic stem-loop probes ligation and SYBR Green real-time PCR

Zeqi Yu[a], Ying Zhu[a], Yunxia Zhang[a], Juan Li[b], Qun Fang[a], Jianzhong Xi[b], Bo Yao[a,*]

[a] Institute of Microanalytical Systems, Department of Chemistry, Zhejiang University, Hangzhou, 310058, China
[b] Department of Biomedical Engineering, College of Engineering, Yan Nan Yuan 60, Peking University, Beijing, 100871, China

ARTICLE INFO

Article history:
Received 30 April 2011
Received in revised form 30 June 2011
Accepted 30 June 2011
Available online 7 July 2011

Keywords:
microRNA
Droplet array
Real-time PCR
Ligation
SYBR Green

ABSTRACT

In this paper, a nanoliter droplet array based on enzymatic stem-loop probes ligation and SYBR Green real-time PCR for quantification of microRNA was developed. By employing T4 RNA ligase 2 instead of T4 DNA ligase, we designed simplified stem-loop probes to perform microRNA-templated DNA ligation and reduced the non-specific ligation of T4 DNA ligase. SYBR green I dye was employed instead of TaqMan probes in present miniaturized real-time PCR systems. Specifically, we optimized the dosage of SYBR Green I dye in nanoliter droplet and verified the performance of this system by detecting synthetic mir-122 with a 6 logs dynamic range (from 1.5×10^5 to 1.5×10^{10} copies). Linear relationship of the standard curve ($R^2 = 0.9997$) and high PCR amplification efficiency (96.83%) were obtained under the optimized conditions. We detected the expression of mir-122 across five mouse tissues and the result was consistent with that TaqMan microRNA assay. We think this miniaturized real-time PCR platform reduced the detection cost considerably, thus showing the great potential to quantitative biology.

1. Introduction

MiRNAs (or microRNAs), encoded by endogenous gene, are small single-stranded, non-coding RNA with the length of 18–25 nucleotides [1]. Its role in regulating gene expression [2,3] has attracted increasing attention in recent years. Plenty of studies revealed that miRNAs participated in a series of important process of life course, including early development [4], cell proliferation [5], cell apoptosis [6]. So, research on accurate, sensitive and low cost miRNA quantification method has great significance for biological research and clinical diagnosis.

However, miRNAs are not easy to detect, because of their small size and high similarity of the sequences. Some conventional methods (i.e. northern blot) [7,8] are complained on low sensitivity, time and labor consuming. At present, real-time reverse transcriptase PCR (real-time RT-PCR) is playing a great role in detecting miRNAs on account of high sensitivity and specificity [9–12]. In order to improve the specificity of miRNA measurement and distinguish single nucleotide mismatch between similar miRNA sequences, real-time RT-PCR assay for miRNA detection always employed stem-loop and TaqMan probe [12] or locked nucleic acid (LNA) modified primers [13]. In addition, it was well known that T4 DNA ligase could efficiently catalyze the joining of 5′-phosphomonoester group and 3′-hydroxyl group of two DNA oligonucleotides in presence of RNA templates [14]. The ligation-dependent assays have been implemented to detect viruses in which two DNA hemi-probes hybridized to viral RNA nucleotides were ligated by T4 DNA ligase, and then used as template for PCR amplification [15,16]. Compared to the conventional PCR based on cDNA reverse transcripted from RNA strands, ligase-mediated gene detection could not only perform precise distinction of RNA sequence variants, but also easily solve the small size limitation of miRNA and produce corresponding DNAs with appropriate length for following PCR amplification. However, T4 DNA ligase was proven catalyzing the connection of single-strand DNA probes at the absence of target molecules [17]. Li et al. [18] proposed a method based on enzymatic stem-loop probes ligation to transform miRNA target into cDNA template. This method significantly reduced the nonspecific ligation of probes and the interference of precursor miRNA and was able to identify a single mutant in the miRNA sequence.

Recently, development of microfabricated platforms has become one of the major trends in chemical and bio-medical applications and numerous researches have been reported on miniaturized PCR technique which has advantages over traditional PCR platform such as high throughput, low cost and low reagent consumption [19,20]. On this basis, we recently developed a low density nanoliter droplet array generated on chemical modified silicon chip for gene quantification [21]. Reliable and sensitive two-step real-time qRT-PCR assay for miRNA measurement was performed within 500 nL droplets. Compared with common continuous-flow-droplet-based PCR system [22,23], it was easy to

* Corresponding author. Tel.: +86 571 88273496; fax: +86 571 88273572.
E-mail address: yaobo08@zju.edu.cn (B. Yao).

0039-9140/$ – see front matter © 2011 Elsevier B.V. All rights reserved.
doi:10.1016/j.talanta.2011.06.075

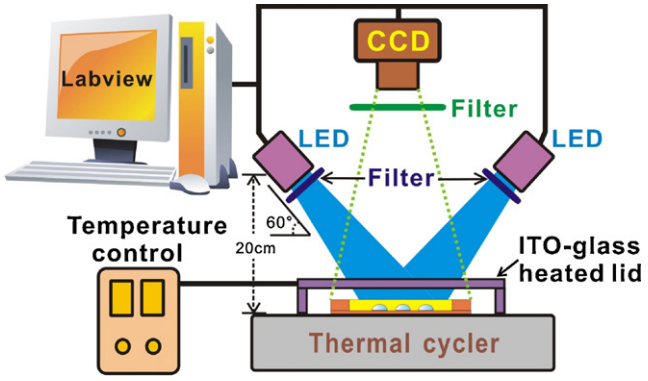

Fig. 1. Schematic illustration of the real-time PCR platform with fluorescence imaging system.

distinguish the fluorescence of immobilized droplets during each thermal cycle. Consequently, parallel assay of different samples and multi-step reactions in droplets was no longer difficult challenge.

To the best of our knowledge, TaqMan probe was used in most of the present microchip-based real-time PCR systems [21,24–27], however SYBR Green based real-time PCR, as an alternative of TaqMan assay, which was usually employed in conventional quantitative PCR was seldom used in miniaturized PCR systems. That might because that oil phase which was usually used to separate droplets and prevent evaporation in present microchip PCR systems would influence and reduce the fluorescence of the complex SYBR Green dye and dsDNA products. Although TaqMan probe could bring about higher sensitivity and ensure the detection specificity, it would increase the experimental cost dramatically. A reliable and inexpensive miniaturized SYBR Green based real-time PCR assay may become more attractive because of its great potential in biological research.

Considering the abovementioned factors, herein, we demonstrated a droplet-based real-time PCR platform utilizing SYBR Green I for miRNA quantification. In this work, we employed T4 RNA ligase 2 instead of T4 DNA ligase in Ref. [18] and special stem-loop probes were designed to minimize non-specific ligation. T4 RNA ligase 2 has better ability to distinguish the specific join-sites than T4 DNA ligase, which makes it much easier to design probes and detect different miRNAs. By using mir-122 as a target mature miRNA, we performed the enzymatic ligation and SYBR Green based real-time PCR and optimized the dosage of SYBR Green dye for fluorescence detection within 500 nL droplet array. We finally validated this method for quantifying the expression of mir-122 across 5 mouse tissues including spleen, kidney, lung, brain and liver.

2. Experimental

2.1. Fabrication of miniature real-time PCR system

The home-made real-time PCR system for microchip fluorescence detection was developed as shown in Fig. 1, including a commercial Thermal Cycler (MGL96G/Y, LongGene, Hangzhou, China) for PCR reaction, two blue light emitting diodes (LED) (3W, Cree, Shenzhen, China) equipped with excitation filter (470D25, HB-Optical, Shenyang, China) as light source and a charge coupled device (CCD) (DH-SV1401FC/FM, Daheng Image, Beijing, China) with magnifying lens (MLM-3XMP, Computar, Tokyo, Japan) and a piece of emission filter (535AF40, Omega, Brattleboro, USA) for fluorescence image capture. The droplet array chip was placed on the metal objective table of the Thermal Cycler. Fabrication method of silicon PCR chips was reported earlier [21]. In brief, we grew a layer of SiO_2 on the surface of the silicon wafer first, and then the surface was silanized to be hydrophobic. After that, a 6 × 6 hydrophilic spot array was fabricated on the surface of the silicon wafer using photolithography followed by wet chemical etching. The transparent indium tin oxide (ITO) glass (1.1 mm thick, 10 ohm, LAIBAO, Shenzhen, China) as heated lid was covered above the PCR chip and its temperature was maintained at 60 °C by a homemade control unit. In addition, a program written in Labview (Labview 8.0, National Instruments, Austin, USA) was used to control two LEDs to open/close, as well as a CCD to acquire fluorescence image of every cycle in real-time and in situ.

2.2. Mature miRNAs, probes, and primers

The sequence of mature mir-122 (UGGAGUGUGACAAUGGUGUUUG) and mir-21 (UAGCUUAUCAGACUGAUGUUGA) selected from the Sanger Center miRBase at http://microrna.sanger.ac.uk/sequences. Synthetic mature miRNA oligonucleotides were synthesized by Shanghai GenePharma (Shanghai, China). Stem-loop probes and primers for mir-122 recognition and PCR amplification were products of Invitrogen (Shanghai, China). The sequence of two probes were: 5′-GGTCGTATCCAGGAGAGGGTGAAGGTATGCGGATTGGATACGACGACAAACACC-3′ (probe1) and 5′-ATTGTCACACTCCAAAGTCGTTCAGGTATAACGACAA-3′ (probe2), respectively. The sequence of forward primer was 5′-GGAGAGGGTGAAGGTATGC-3′ and the reverse primer was 5′-TGAACGACTTTGGAGTGTGA -3′.

2.3. Tissue preparation and total RNA extraction

Dissected organs including spleen, kidney, lung, brain and liver from 3-week-old ICR mice provided by Zhejiang University Laboratory Animal Center (Hangzhou, China), were used for preparing mouse total RNA samples. All animal procedures were in accordance with Institutional Animal Care and Use Committee (IACUC) and OECD guidelines. Total RNA was extracted using TRNzol (Tiangen, Beijing, China) according to the manufacturer's protocol and the concentration of total RNA was quantified by the value of A260 on a SP-752TM UV–vis spectrophotometer (Spectrum Shanghai, China).

2.4. Ligation reaction

First, probe 2 was phosphorylated as follows. 10 μL of 100 μM of probe 2 incubated at 75 °C for 5 min, then placed on ice for 2 min. The phosphorylation reaction was performed in a 20 μL volume containing aforementioned probe 2, 20 nmol of rATP (Promega, Beijing, China), 10 U of T4 Polynucleotide kinase (T4PNK) (TaKaRa, Dalian, China) and 2 μL of T4PNK buffer at 37 °C for 2 h, 65 °C for 20 min.

After phosphorylation, 50 pmol of probe 1 and 50 pmol of 5′-phosphorylated probe 2, 2 μL of sample solution (synthetic miRNA or isolated total RNA) and 12 U of Cloned Ribonuclease Inhibitor (RRI) (TaKaRa, Dalian, China) were mixed together and fixed up to 3.8 μL of anneal volume with DEPC treated water. The mixture was incubated at 65 °C for 3 min, then slowly cooled down to 25 °C. 2.5 U of T4 RNA ligase 2 (New Eanland Biolabs, Beijing, China), 0.5 μL of 10 × ligation buffer was added into the above mixture to a final volume of 5 μL. When using T4 DNA ligase, 175 U of T4 DNA ligase (TaKaRa, Dalian, China), 0.2 μL of RRI, and freshly prepared buffer of 50 nmol Tris–HCl pH 7.5, 50 nmol $MnCl_2$, 50 pmol ATP, 500 pmol DTT (TaKaRa, Dalian, China) was added into the above mixture to a final volume of 5 μL. 150 nL of ligation solution would be spotted on one hydrophilic spot area by using pipette (0.1–2.5 μL Research®, Eppendorf, Shanghai, China). When the whole 6 × 6 droplet array had been spotted, 200 μL of PCR mineral oil (Sigma–Aldrich, St. Louis, USA) was covered the whole array to prevent droplet evap-

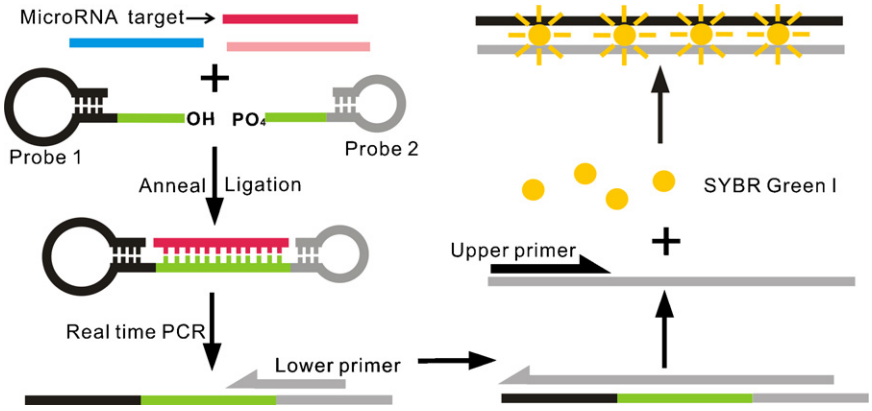

Fig. 2. Schematic diagram of stem-loop probes ligation-based real-time PCR assay for detection of miRNAs. A couple of oligonucleotide stem-loop probes (probe 1 and probe 2) were designed to hybridize with target miRNA. Then the probes were annealed and ligated in the presence of T4 RNA ligase 2. The joint DNA strand was used as a template in the following PCR amplification. Quantification was performed on self-made droplet-based real-time PCR system utilizing SYBR Green I as the quantitative dye.

oration. Finally, the PCR chip incubated at 37 °C for 2 h (for T4 RNA ligase 2), or 16 °C 1.5 h, 70 °C 20 min (for T4 DNA ligase), respectively.

2.5. SYBR Green real-time PCR assay

After ligation, each droplet would be added with 350 nL PCR premix containing 250 nL of SYBR® Premix Ex Taq™ (TaKaRa, Dalian, China), 50 nL of 10 μM forward and reverse primers and 15 nL of 20 × SYBR Green I (Biovision, Xiamen, China). The PCR reaction was performed at 95 °C for 2 min, followed by 35 cycles of 94 °C for 30 s, 60 °C for 40 s and 72 °C for 30 s. The fluorescence image of each cycle was acquired during the extension segment at 72 °C by CCD camera.

2.6. Data processing methodology

For data analysis, the fluorescence intensity of each droplet was read out using a program written in Labview and translated into amplification plot using Excel and Origin. The threshold cycle (Ct) was defined as the fractional cycle number at which the relative fluorescence intensity became greater than the threshold where the threshold was defined as 10-fold of the standard deviation (SD) value of the PCR plot baseline.

3. Results and discussion

3.1. Choice of ligase

T4 DNA ligase was proven to be able to distinguish a single mismatch from nucleotide sequence homologous to target miRNA, however, Li et al. found that T4 DNA ligase could also catalyze the ligation between 5′-phosphomonoester and 3′-hydroxyl group of single DNA strands in the absence of miRNA targets [18], albeit with substantially lower ligation yield. Those nonspecific background signals would be significantly intensified in the subsequent PCR amplification, thus becoming a very serious problem when low-abundant miRNA target was characterized. In order to resolve this problem, a couple of improved probes with a stem-loop structure were designed, however, which might bring the increment difficulty for probe design. Meanwhile, T4 RNA ligase 2 was also a kind of enzyme, which could efficiently catalyze the ligation of RNA-templated DNA fragments [28,29]. Cheng et al. also demonstrated that T4 RNA ligase 2 can greatly improve the specificity for the ligation of padlock probes by using miRNA as the template and sensitively detected miRNA through a branched rolling-circle amplification (BRCA) reaction [30].

In this work, we employed T4 RNA ligase 2 to catalyze miRNA-templated DNA ligation, instead of T4 DNA ligase in Ref. [18]. The schematic diagram of this method was shown in Fig. 2, including hybridization, ligation and PCR amplification steps. Obviously, the ligation of two DNA probes was the key step where ligase was necessary to catalyze the joining of 5′-phosphomonoester group and 3′-hydroxyl group of two probes in the presence of miRNA target as template. To investigate the specificity of the miRNA-templated ligation assay, we compared the catalysis efficiency between T4 DNA ligase and T4 RNA ligase 2. Fig. 3 shows the difference of cycle threshold value (ΔCt) of the two ligase. For T4 DNA ligase, the fluorescence of all droplets enhanced quickly and almost simultaneously. The ΔCt between mir-122/mir-21 and no template control (NTC) were very slight (only about 0.7 and 1.9 cycles) at a concentration of 1.5×10^8 copies per droplet. This result verified that even without target sequence, T4 DNA ligase could still get two nucleotide probes (probe1 and probe2 in Fig. 2) joining together nonspecifically [18]. However, when using T4 RNA ligase 2, the Ct value of mir-122 was significantly different from that of NTC, while the fluorescence of mir-21 remained unchanged until the fluorescence of NTC started to increase at about the 27th cycle. It meant that T4 RNA ligase 2 could catalyze stem-loop probes ligation only in the presence of specific target sequence. ΔCt between mir-122 and NTC ($Ct_{mir\text{-}122} - Ct_{NTC}$) was evidently increased when the T4 RNA ligase 2 was employed compared to T4 DNA ligase (about 12.1 vs. 1.9 cycles), thus reducing the nonspecific ligation at least 1000

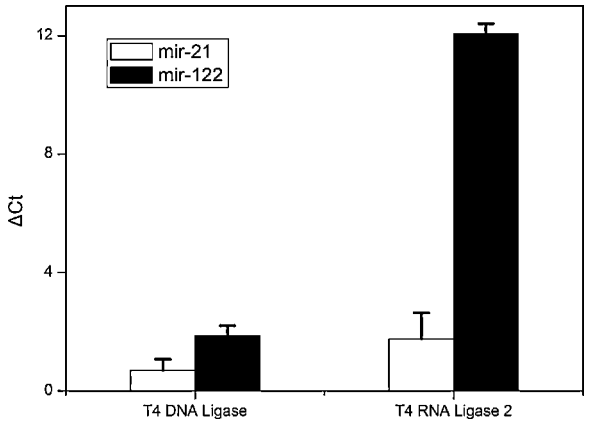

Fig. 3. Histogram of the difference of Ct value (ΔCt) between mir-122/mir-21 and no template control (NTC) across two ligases.

folds in our work, which was significantly improved compared with previous BRCA method [30].

3.2. Optimization of dosage of SYBR Green I

In addition to TaqMan assay, the SYBR Green PCR assay is another commonly used real-time PCR technique, which is employed by most of the researchers. SYBR Green PCR is widely used because of the ease in designing the assays and its relatively low setup and running costs. Despite its widespread use, this technique was surprisingly seldom reported in miniaturized PCR systems. Although the commercial kit used in our real-time PCR detection system contained certain concentration of SYBR Green I dye, we found that the fluorescence intensity of the droplets hardly increased during PCR amplification even at high concentration of template. We think that might be mainly caused by the influence of the mineral oil covered on the droplet array for preventing evaporation. In this experiment it was observed that the concentration of SYBR Green I was critical for the relative fluorescence intensity of small volume PCR amplification in droplet, affecting not only the sensitivity but also the Ct value. Fig. 4 shows that the amount of SYBR Green I put into the PCR mixture would greatly affect the ΔCt value, as well as relative fluorescence intensity at the plateau phase (at 40th cycle) of amplification.

It was observed that, the ΔCt ($Ct_{mir\text{-}122} - Ct_{NTC}$) increased with the increment dye concentration before 15 nL/droplet of SYBR Green I input, while greatly decreased when the input amount was above 15 nL/droplet. Meanwhile, relative fluorescence intensity at the plateau phase increased with the concentration of extra SYBR Green I, and increase rate decreased gradually. Nevertheless, when the concentration of extra SYBR Green I was above 30 nL/droplet, relative fluorescence intensity dropped rapidly. We think that is a balance of two kinds of influence of the SYBR Green dye on the droplet array based real-time PCR assay, one is the increment of sensitivity of the fluorescence detection and the other is the inhibition of the PCR amplification [31]. Therefore considering of the ΔCt and relative fluorescence intensity synthetically, 15 nL/droplet of extra SYBR Green I was used as an optimized concentration for high sensitivity of the droplet array based real-time PCR assay.

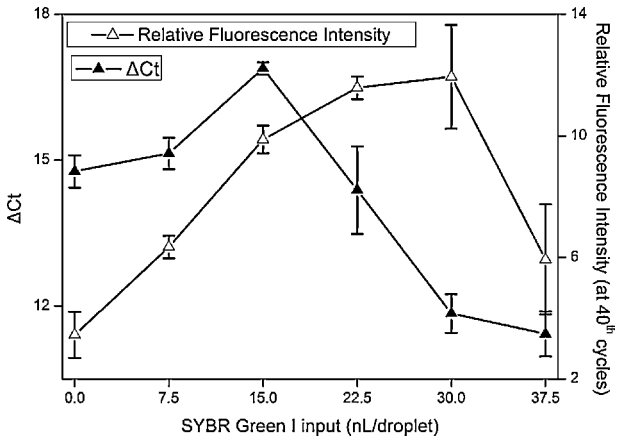

Fig. 4. Correlation of the amount of SYBR Green I put into the PCR mixture to the ΔCt value and the relative fluorescence intensity at the 40th cycle. There were 6 groups with 0, 7.5, 15, 22.5, 30, 37.5 nL of extra SYBR Green I put into the 500 nL droplets, respectively. Each group was tested in 6 independent droplets where 3 droplets contained 1.5×10^8 copies of mir-122 and the other 3 droplets were no template control.

3.3. Performance of the droplet based PCR assay

We used synthetic mir-122 to test the performance of this droplet array based SYBR Green real-time quantitative PCR assay. Fig. 5a shows the distribution of different droplet reactions and a series of fluorescence images of droplets with serial dilution of synthetic mir-122 (from 1.5×10^5 to 1.5×10^{10} copies) at different

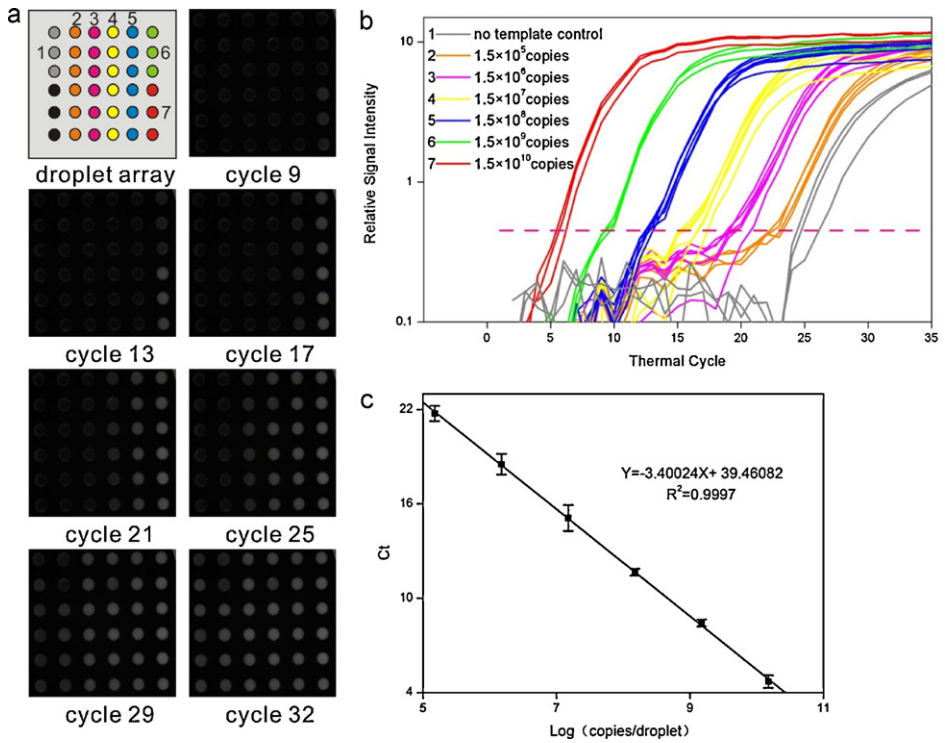

Fig. 5. Real-time quantitative PCR detection of synthetic mir-122: (a) distribution of droplet array and the fluorescence images at different thermal cycles. The input of synthetic mir-122 is 1.5×10^{10}, 1.5×10^9, 1.5×10^8, 1.5×10^7, 1.5×10^6, 1.5×10^5 and 0 copies per droplet, respectively. Each reaction was run in triplicate or sextuplicate. (b) Amplification plot of synthetic mir-122 over six orders of magnitude. (c) Standard curve of synthetic mir-122.

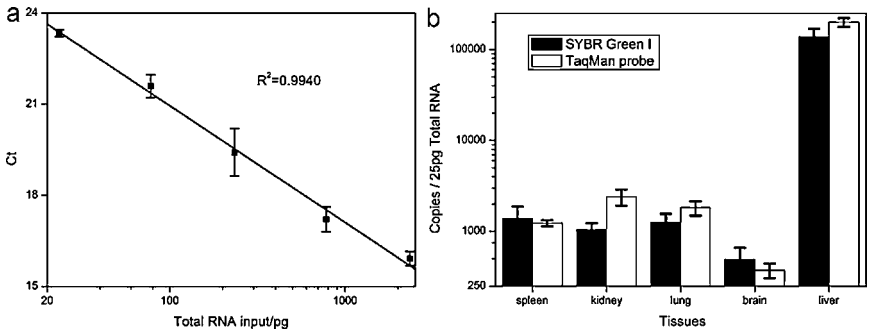

Fig. 6. (a) Correlation of total RNA input (23.4–2340 pg/500 nL droplet) to the Ct values of mir-122 in mouse liver. (b) Relative expression profiles of mir-122 across 5 kinds of mouse tissues. The dark and white rectangles represent the relative expression of mir-122 detected by our system using SYBR Green I and real-time RT-PCR system using TaqMan probes, respectively. Both of them show high expression of mir-122 in liver, and low expression in other tissues.

thermal cycles. The amplification plot was given in Fig. 5b. Plotting the Ct value against the logarithm of copy number of synthetic mir-122 input (shown in Fig. 5c), excellent linear relationship was obtained (R^2 = 0.9997). It meant a dynamic range of at least 6 logs was available in a single assay with this system. At the same time, amplification efficiency reached as much as 96.83%.

3.4. Expression profile of mir-122 in tissues

As mir-122 is specifically abundant in the adult liver tissue and it constitutes 70% of the total miRNA population [32], next we tested the capability of this assay to detect changes in mir-122 expression across 5 tissues isolated from 3-week-old ICR mice. Total RNA extracted from spleen, kidney, lung, liver and brain was quantified based on the A260 value. In 500 nL droplet, for liver tissues in which the expression of mir-122 was highest, the linear correlation (R^2 = 0.9940) of the Ct value to total RNA input (23.4–2340 pg) was shown in Fig. 6a. Actually, it was found that PCR amplification would be inhibited notably if total RNA input was above 2340 pg per droplet, which caused the increment of fluorescence intensity too weak to be detected. Therefore, the total RNA input should be ensured within the linear range to obtain high sensitivity and accuracy.

Furthermore, we investigated the expression of mir-122 in mouse liver and other 4 tissues. As showed in Fig. 6b, the result was consistent with that of real-time RT-PCR system based on nanoliter droplet array employing TaqMan probe [21], thus proving the ability of this system to detect real biological sample. As expected, mir-122 was highly expressed in mouse liver, but extremely low in other tissues, which was in agreement with that reported in earlier literature [33].

4. Conclusions

In summary, we developed a SYBR Green real-time PCR system for quantification of miRNAs based on stem-loop probes ligation and nanoliter droplet array. This platform has several advantages including: (1) the utilization of nanoliter droplet array reduced the reagent/sample consumption greatly from over 10 μL to 500 nL; (2) the implementation of PCR chip based on silicon chip realized multi-step and parallel reactions in droplets which were used as immobilized micro-reactors; (3) employing T4 RNA ligase 2 which greatly improved the specificity of the assay through reducing the non-specific ligation of T4 DNA ligase in miRNA-templated DNA probes ligation reaction; (4) it was demonstrated that SYBR Green dye could also be successfully used in miniaturized real-time PCR assay. The whole detection system was very easy to be constructed, which might be helpful for widely application. We believe this system might become a simple, sensitive, accurate and especially low cost tool for detection of miRNAs, even could be employed for large-scale actual application.

Acknowledgments

This work was supported by the National Natural Science Foundation of China (no. 20905064 and no. 20890020), the Research Fund for the Doctoral Program of Higher Education of China (20090101120007), Zhejiang Provincial Natural Science Foundation of China (Y409002) and Chinese Universities Scientific Fund (KYJD09001). The authors thank Prof. Ying Mu Zhejiang University for RNA storage.

References

[1] M. Lagos-Quintana, R. Rauhut, W. Lendeckel, T. Tuschl, Science 294 (2001) 853–858.
[2] B.P. Lewis, I.H. Shih, M.W. Jones-Rhoades, D.P. Bartel, C.B. Burge, Cell 115 (2003) 787–798.
[3] N.C. Lau, L.P. Lim, E.G. Weinstein, D.P. Bartel, Science 294 (2001) 858–862.
[4] E. Wienholds, W.P. Kloosterman, E. Miska, E. Alvarez-Saavedra, E. Berezikov, E.D. Bruijn, H.R. Horvitz, S. Kauppinen, R.H.A. Plasterk, Science 309 (2005) 310–311.
[5] T.H. Thai, D.P. Calado, S. Casola, K.M. Ansel, C.C. Xiao, Y.Z. Xue, A. Murphy, D. Frendewey, D. Valenzuela, J.L. Kutok, M. Schmidt-Supprian, N. Rajewsky, G. Yancopoulos, A. Rao, K. Rajewsky, Science 316 (2007) 604–608.
[6] L. He, J.M. Thomson, M.T. Hemann, E. Hernando-Monge, D. Mu, S. Goodson, S. Powers, C. Cordon-Cardo, S.W. Lowe, G.J. Hannon, S.M. Hammond, Nature 435 (2005) 828–833.
[7] E. Berezikov, V. Guryev, J.V.D. Belt, E. Wienholds, R.H.A. Plasterk, E. Cuppen, Cell 120 (2005) 21–24.
[8] R.C. Lee, R.L. Feinbaum, V. Ambros, Cell 75 (1993) 843–854.
[9] U.E.M. Gibson, C.A. Heid, P.M. Williams, Genome Res. 6 (1996) 995–1001.
[10] A. Giulietti, L. Overbergh, D. Valckx, B. Decallonne, R. Bouillon, C. Mathieu, Methods 25 (2001) 386–401.
[11] A.J. Qavi, J.T. Kindt, R.C. Bailey, Anal. Bioanal. Chem. 398 (2010) 2535–2549.
[12] C. Chen, D.A. Ridzon, A.J. Broomer, Z.H. Zhou, D.H. Lee, J.T. Nguyen, M. Barbisin, N.L. Xu, V.R. Mahuvakar, M.R. Andersen, K.Q. Lao, K.J. Livak, K.J. Guegler, Nucl. Acids Res. 33 (2005) e179.
[13] C.K. Raymond, B.S. Roberts, P. Garrett-Engele, L.P. Lim, J.M. Johnson, RNA 11 (2005) 1737–1744.
[14] K. Kleppe, J.H.V.D. Sande, H.G. Khorana, Proc. Natl. Acad. Sci. U.S.A. 67 (1970) 68–73.
[15] Y.N. Park, K. Abe, H.B. Li, T. Hsuih, S.N. Thung, D.Y. Zhang, Am. J. Pathol. 149 (1996) 1485–1491.
[16] T.C. Hsuih, Y.N. Park, C. Zaretsky, F. Wu, S. Tyagi, F.R. Kramer, R. Sperling, D.Y. Zhang, J. Clin. Microbiol. 34 (1996) 501–507.
[17] H. Kuhn, M.D. Frank-Kamenetskii, FEBS J. 272 (2005) 5991–6000.
[18] J. Li, B. Yao, H. Huang, Z. Wang, C.H. Sun, Y. Fan, Q. Chang, S.L. Li, X. Wang, J.Z. Xi, Anal. Chem. 81 (2009) 5446–5451.
[19] P.A. Auroux, Y. Koc, A. Demello, A. Manz, P.J.R. Day, Lab Chip 4 (2004) 534–546.
[20] K.Y. Lien, G.B. Lee, Analyst 135 (2010) 1499–1518.
[21] Y.X. Zhang, Y. Zhu, B. Yao, Q. Fang, Lab Chip 11 (2011) 1545–1549.
[22] M.U. Kopp, A.J.D. Mello, A. Manz, Science 280 (1998) 1046–1048.
[23] M. Hashimoto, P.C. Chen, M.W. Mitchell, D.E. Nikitopoulos, S.A. Soper, M.C. Murphy, Lab Chip 4 (2004) 638–645.
[24] N.R. Beer, E.K. Wheeler, L. Lee-Houghton, N. Watkins, S. Nasarabadi, N. Hebert, P. Leung, D.W. Arnold, C.G. Bailey, B.W. Colston, Anal. Chem. 80 (2008) 1854–1858.
[25] S.L. Spurgeon, R.C. Jones, R. Ramakrishnan, PloS ONE 3 (2008) e1662.

[26] Q. Xiang, B. Xu, R. Fu, D. Li, Bimoed. Microdevices 7 (2005) 273–279.
[27] Q. Xiang, B. Xu, D. Li, Bimoed. Microdevices 9 (2007) 443–449.
[28] X.H. Zhang, V.L. Chiang, Nucl. Acids Res. 24 (1996) 990–991.
[29] D.M. Hinton, J.A. Baez, R.I. Gumport, Biochemistry 17 (1978) 5091–5097.
[30] Y.Q. Cheng, X. Zhang, Z.P. Li, X.X. Jiao, Y.C. Wang, Y.L. Zhang, Angew. Chem. Int. Ed. 48 (2009) 3268–3272.
[31] K. Nath, J.W. Sarosy, J. Hahn, C.J.D. Como, J. Biochem. Biophys. Methods 42 (2000) 15–29.
[32] C.L. Jopling, M.K. Yi, A.M. Lancaster, S.M. Lemon, P. Sarnow, Science 309 (2005) 1577–1581.
[33] J.H. Chang, E. Nicolas, D. Marks, C. Sander, A. Lerro, M.A. Buendia, C.X. Xu, W.S. Mason, T. Moloshok, R. Bort, K.S. Zaret, J.M. Taylor, RNA Biol. 1 (2004) 106–113.